J. Fluid Mech. (2011), *vol.* 688, *pp.* 591–601.
doi:10.1017/jfm.2011.408

Scaling the circulation shed by a pitching panel

James H. J. Buchholz[1]†, Melissa A. Green[2] and Alexander J. Smits[3]

[1] Department of Mechanical and Industrial Engineering / IIHR – Hydroscience & Engineering, University of Iowa, Iowa City, IA 52242, USA

[2] Laboratories for Computational Physics and Fluid Dynamics, Naval Research Laboratory, Washington, DC 20375, USA

[3] Department of Mechanical and Aerospace Engineering, Princeton University, Princeton, NJ 08544, USA

(Received 23 May 2011; revised 8 September 2011; accepted 20 September 2011; first published online 31 October 2011)

A new scaling parameter is developed for the circulation shed by a rigid, rectangular panel pitching periodically about its leading edge. This parameter is the product of a kinematic and a geometric component. The kinematic component describes the relationship between the mean vorticity flux from the panel surface and the panel motion. The geometric component depends on the ratio of pitching amplitude to the span of the panel. The kinematic component is developed based on the connection between the surface pressure distribution and the resulting surface vorticity flux, which are supported in a stroke-averaged sense by pressure measurements on the surface of the panel. The parameter gives a robust scaling for the total spanwise circulation shed in a half-cycle by the panel. It provides a useful predictive tool, in that it can be either complementary to the formation number or provide an alternative scaling parameter when vortex saturation and pinch-off do not occur.

Key words: propulsion, swimming/flying, vortex shedding

1. Introduction

It is well known that a wing or fin oscillating in a pitching and/or heaving motion can produce a thrust force on the body (Koochesfahani 1989; Anderson *et al.* 1998). Bodies of high aspect ratio will generate a nominally two-dimensional reverse von Kármán street under conditions of efficient thrust production (Triantafyllou, Triantafyllou & Yue 2000) and low-aspect-ratio bodies will generate a highly three-dimensional wake (Dong, Mittal & Najjar 2006; Buchholz & Smits 2006, 2008; Borazjani & Sotiropoulos 2010). Wake dynamics can impact the thrust performance of oscillating foils, and reflect the forcing history of the body (Young & Lai 2007). Therefore, qualitative and quantitative descriptions of the wakes shed by oscillating wings can provide insight into the physical mechanisms of force generation, which can then lead to improved models for the design of biomimetic propulsors for underwater vehicles and fish habitat structures, and also provide a useful characterization of the local environment experienced by agents swimming or flying in groups.

Here we examine the spanwise circulation shed by a rectangular panel pitching about its leading edge. Buchholz & Smits (2008) demonstrated that the vortex

† Email address for correspondence: james-h-buchholz@uiowa.edu

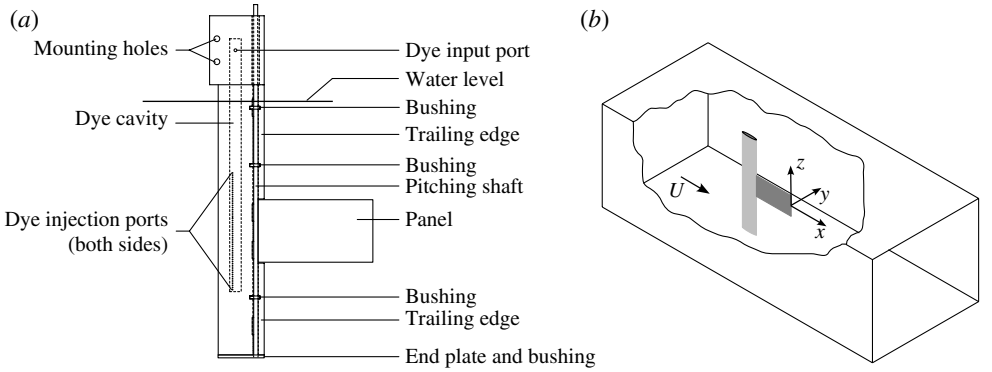

FIGURE 1. (*a*) The fairing and panel assembly. (*b*) Orientation in the water channel and coordinate system definition. These images appear in Buchholz & Smits (2008).

topology of the wake is robust with respect to Reynolds number, Strouhal number, and geometric parameter variations, and that it bears a striking resemblance to a broad range of low-aspect-ratio unsteady wakes. This qualitative generality of the wake suggests that a similarity parameter for wake circulation may also exist. If such a parameter can be found and generalized to other geometries and kinematics, it will provide an important tool for the prediction of force augmentation by vortex shedding, and elucidate quantitative aspects of the wakes of unsteady wings and fins. We propose such a parameter, composed of the product of a non-dimensional circulation and a geometric scaling. This new parameter has a nearly constant value for low-aspect-ratio panels with varying Strouhal number, aspect ratio, and pitching amplitude. The physics of parameter variation are discussed, and its application is considered in the context of vortex formation number.

2. Experimental methods

This investigation extends the work of Buchholz & Smits (2006, 2008) and Green & Smits (2008), where further details of the experiments may be found. Experiments were conducted in a water channel of width 0.46 m, depth 0.29 m and length 2.44 m with flow conditioning consisting of a 5:1 contraction, honeycomb flow straightener and screens. The experimental setup in the water channel is shown in figure 1(*b*), which also defines the coordinate system. Three rigid rectangular panel propulsors were investigated with aspect ratios $AR = S/C = 0.54$, 0.83 and 2.38 (where S is the panel span and $C = 120$ mm is the chord). The highest aspect ratio may be considered a quasi-two-dimensional case since it spanned the depth of the water channel to within 5 mm of the bottom and top surfaces (an acrylic plate was placed on the water surface to prevent free surface effects that could affect the flow dynamics and visualization). Each panel was pitched about its leading edge by a pitching shaft located near the trailing edge of a stationary, modified NACA 0012-64 aerofoil, as shown in figure 1(*a*). The Reynolds numbers based on the chord length C of the panel $Re_C = U_\infty C/\nu$ were of $O(10^4)$, where U_∞ is the free-stream velocity and ν is the kinematic viscosity of the fluid. The Strouhal number was varied by modifying the free-stream velocity while keeping the pitching frequency constant. Here, the Strouhal number is $St = fA/U_\infty$, where f is the pitching frequency, and A is the peak-to-peak pitching amplitude of the trailing edge. The combinations of panel aspect ratio, and pitching amplitude are

Designation	S (mm)	C (mm)	A (mm)	$AR = S/C$	A/S
P1A2	65	120	20	0.54	0.31
P1A3.1	65	120	31	0.54	0.48
P1A4	65	120	40	0.54	0.62
P2A2	100	120	20	0.83	0.20
P2A3.1	100	120	31	0.83	0.31
P4A3.1	286	120	31	2.38	0.11

TABLE 1. Summary of panel aspect ratio and pitching amplitude combinations, and case designations. Cases are named according to panel number and pitching amplitude. For example, P1A2 is panel 1 pitched with a peak-to-peak trailing edge amplitude of 20 mm.

summarized in table 1, where panel numbers (P1, P2, P4) are chosen to conform with the notation used by Buchholz & Smits (2008).

The flow field was interrogated using digital particle image velocimetry (DPIV) on the horizontal symmetry plane of each panel. Details of the DPIV system and its application are given by Buchholz & Smits (2008). Two-dimensional, two-component velocity fields were computed by conducting local spatial cross-correlations on corresponding 64×64 and 32×32 pixel windows with 50 % overlap, to produce $128 \times 128 = 16384$ vectors. Phase averaging was achieved by using a rotary encoder mounted to the pitching shaft to trigger data acquisition at the desired panel position. Phase-averaged vorticity distributions presented here are generated from 30 velocity fields unless otherwise noted.

Surface pressure distributions on the panel were measured at discrete chordwise positions on the symmetry line of the panel using a Validyne DP-15 differential pressure transducer with one port connected to a pressure port on the panel surface and the other port open to the atmosphere. Green & Smits (2008) provide further details. All pressure measurements reported here are relative to a baseline measurement with no flow in the water channel and no motion of the panel (that is, hydrostatic pressure), and they were phase-averaged over (typically) 28 cycles.

3. Results

Spanwise vorticity fields, derived from DPIV measurements on the symmetry plane, were used to make qualitative observations of wake patterns, and to compute the circulation of spanwise vorticity shed from the trailing edge.

3.1. *Wake circulation*

At $Re_C = O(10^4)$, spanwise vorticity was shed from the trailing edge in the form of a discrete vortex structure often followed by a more elongated structure (shear-layer-like), or a train of discrete vortices resulting (presumably) from a Kelvin–Helmholtz-like instability. For the low-aspect-ratio panels, the wake bifurcated to produce two streams of transversely oriented, counter-rotating vortex pairs, as shown in figures 2(*a*) and 2(*b*). For the high-aspect-ratio panel, a reverse von Kármán street was observed (figure 2*c*).

The circulation Γ shed in one stroke (one half-cycle) of period T is defined from phase-averaged realizations at $t/T = 0$ such that the panel is parallel to the free stream and the trailing edge is moving in the positive y-direction. The vorticity shed in the previous half-cycle is considered because it is detached from the panel but it has not

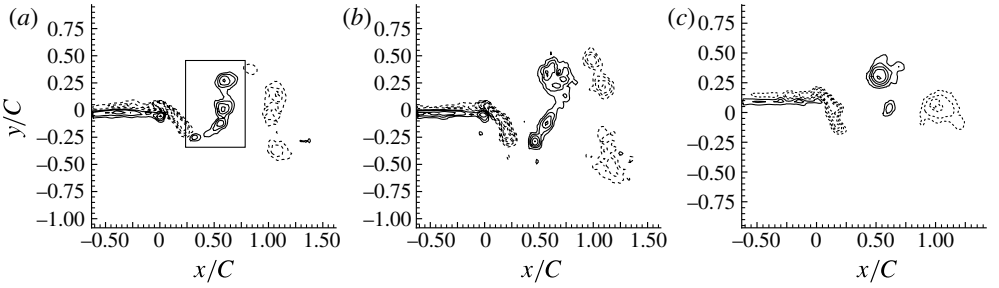

FIGURE 2. Vorticity contours in the wake of pitching panels. (*a*) $AR = 0.54$, $A/S = 0.31$, $St = 0.17$, $Re_C = 28,200$; (*b*) $AR = 0.54$, $A/S = 0.48$, $St = 0.27$, $Re_C = 27,600$; (*c*) $AR = 2.38$, $A/S = 0.11$, $St = 0.36$, $Re_C = 7,200$. Contour values are $\pm n^2\ \mathrm{s}^{-1}$, $n = 2, 3, 4, \ldots, 10$.

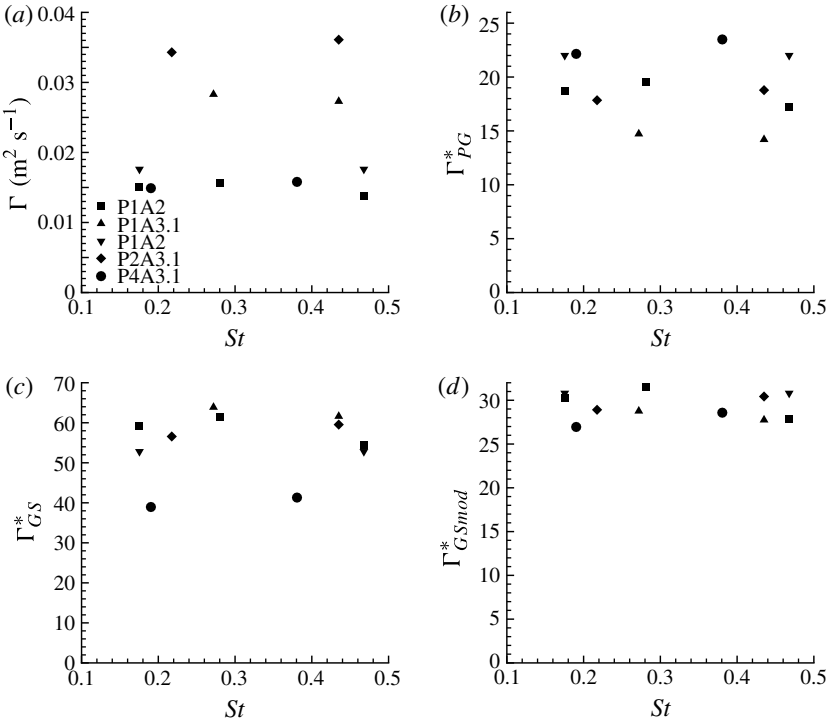

FIGURE 3. Wake circulation values: (*a*) raw dimensional data; (*b*) non-dimensionalized according to (3.3); (*c*) non-dimensionalized according to (3.5) with $\beta = 7$; (*d*) non-dimensionalized according to (3.5) with $\beta = 2$.

had time to significantly diffuse and be annihilated through interactions with adjacent structures. Figure 2(*a*) shows a box surrounding a representative structure of interest. The circulation is calculated by numerical quadrature of the vorticity distribution above a vorticity threshold of 1 s^{-1}, as in Buchholz & Smits (2008). The result was found to be insensitive to the threshold, and the uncertainty in the circulation measurements is estimated to be approximately 5 %.

Figure 3(*a*) shows dimensional circulation values for the cases summarized in table 1 as a function of Strouhal number. Because the Strouhal number is varied by

changing the free-stream velocity, figure 3(*a*) shows that the circulation is insensitive to free-stream velocity within the investigated parameter range, and thus depends primarily on the panel geometry and kinematics. The low-aspect-ratio panels with small pitching amplitude (P1A2, P2A2) have lower circulation values than those with higher pitching amplitude (P1A3.1, P2A3.1). The circulation values of the high-aspect-ratio panel (P4A3.1) are similar to those of the low-aspect-ratio, low-amplitude panels. In the following discussion, we will consider the scaling of all these data, although we will focus primarily on the performance of panels P1 and P2.

3.2. *Kinematic scaling of circulation*

Physical constraints exist that can help guide the development of a similarity parameter to scale the circulation data. For periodic oscillation, for example, the circulation shed in one oscillation cycle must equal the net circulation generated in that same period. Thus, in accordance with Kelvin's circulation theorem, a change in the bound circulation must result in the shedding of vorticity of equal strength and opposite sign. This suggests an unsteady aerodynamic model for the circulatory lift (see, for example, Theodorsen 1935). Alternatively, we may consider the flux of vorticity from the panel. A streamwise pressure gradient along a viscous wall will result in a flux of spanwise vorticity at the surface with magnitude given by (Lighthill 1963)

$$-\nu\frac{\partial\omega_z}{\partial y} = -\nu\frac{\partial}{\partial y}\left(\frac{\partial v}{\partial x} - \frac{\partial u}{\partial y}\right) \approx \nu\left(\frac{\partial^2 u}{\partial y^2}\right) = \nu\nabla^2 u = \frac{1}{\rho}\frac{\partial p}{\partial x}. \tag{3.1}$$

Wu & Wu (1993, 1996) extended this work to arbitrarily moving boundaries:

$$-\nu(\boldsymbol{n}\cdot\nabla\boldsymbol{\omega}) = -\boldsymbol{n}\times\frac{\nabla p}{\rho} - \boldsymbol{n}\times\boldsymbol{a} + (\boldsymbol{n}\times\boldsymbol{\tau}_w)\cdot\boldsymbol{K} + \boldsymbol{n}\{\boldsymbol{n}\cdot(\nabla\times\boldsymbol{\tau}_w)\}, \tag{3.2}$$

where $\boldsymbol{n}$ is the wall normal vector, $\boldsymbol{a}$ is the acceleration of the boundary, $\boldsymbol{\tau}_w$ is the wall shear stress, and $\boldsymbol{K}$ is the wall curvature. Panel kinematics dictate that $\boldsymbol{n}\times\boldsymbol{a}\approx 0$ everywhere on the panel surface, and since there is no surface curvature the second and third terms on the right side of (3.2) vanish. The fourth term on the right describes the introduction of wall-normal vorticity by rotation of vorticity initially parallel to the boundary, and because we are only concerned with spanwise vorticity this term is not relevant. Hence, pressure gradients are expected to be the dominant source of spanwise vorticity on the surface of the panel.

Given the insensitivity of circulation to free-stream velocity, the aggregate streamwise pressure gradients on the panel may also be insensitive to free-stream velocity and depend primarily on panel geometry and kinematics. A kinematic scaling may therefore be based on the dynamic pressure associated with the maximum transverse velocity of the panel, proportional to fA for small angles. The resulting vorticity flux occurs over a time proportional to the period of motion $1/f$, so that we arrive at a non-dimensional circulation given by

$$\Gamma^*_{PG} = \frac{\Gamma}{(fA)^2\,\frac{1}{f}} = \frac{\Gamma}{fA^2}. \tag{3.3}$$

The dimensionless circulation data are significantly compressed compared with the dimensional data, as shown in figure 3(*b*). The effectiveness of the parameter can be quantified by considering the normalized standard deviation of the circulation $\overline{\sigma_\Gamma} = \sigma_\Gamma/\overline{\Gamma}$. For the dimensional data of figure 3(*a*), the low-aspect-ratio panels (P1 and P2) yield $\overline{\sigma_\Gamma} = 0.38$, whereas $\overline{\sigma_\Gamma} = 0.15$ after scaling the data according to (3.3).

3.3. *Geometrical considerations*

The failure of (3.3) to fully collapse the circulation data might be expected since the scaling addresses only kinematics, and not geometry. Figure 3(*b*) reveals a distinct inverse relationship between the non-dimensional circulation and the ratio A/S reported in table 1. Buchholz & Smits (2008) showed that the quantity A/S was an important parameter governing the propulsive efficiency and suggested that it is essentially an aspect ratio of the wake such that, for small A/S, two-dimensional interactions between spanwise vortices dominate, whereas for larger A/S self-induction of individual structures becomes more important to wake dynamics. Green & Smits (2008) further elucidated the role of A/S based on pressure measurements on panels of two different aspect ratios. In particular, they developed a similarity parameter for the pressure coefficient given by

$$C_P{}^* = C_P \left(1 + \beta \frac{A}{S}\right), \tag{3.4}$$

where C_P is the coefficient of pressure such that $C_P = \Delta p/(1/2)\rho U^2$, Δp is the peak-to-peak amplitude of the pressure variation, and $\beta = 7$. They found this scaling to also collapse the thrust coefficient data of Buchholz & Smits (2008).

Expressing (3.3) in the form of (3.4) yields

$$\Gamma^*_{GS} = \Gamma^*_{PG} \left(1 + \beta \frac{A}{S}\right). \tag{3.5}$$

Figure 3(*c*) demonstrates that this scaling is highly effective in collapsing the low-aspect-ratio data ($\overline{\sigma_\Gamma} = 0.070$, and the mean value $\overline{\Gamma^*}_{GS} = 58.0$), although the high-aspect-ratio values are distinct from those of the low-aspect-ratio panels. However, by putting $\beta = 2$ in (3.5), the scaling also collapses the panel P4 data, as figure 3(*d*) shows. In this case, $\overline{\sigma_\Gamma} = 0.046$, which is within the experimental error. It should be noted that several other scaling parameters were tested, including a kinematic parameter based on the bound circulation variation predicted by Theodorsen's theory (Theodorsen 1935), a formation number proposed by Dabiri (2009) and other plausible variable combinations. These parameters were all found to be less effective in collapsing the circulation data than (3.5). The relation between (3.5) and Dabiri's formation number formulation is further discussed in § 4.3.

4. Discussion

Here, we explore the physical basis for (3.5) and provide further evidence of its robustness. The parameter is then discussed in the context of vortex formation number.

4.1. *Physical basis for the circulation scaling*

In §§ 3.2 and 3.3 it was shown that the circulation is insensitive to free-stream velocity, and therefore depends primarily on the kinematics and geometry of the panel. Similar measurements at $Re_C = 640$ (not shown), where St is modified by varying pitching frequency while keeping the free-stream velocity constant, reveal an almost linear relationship between circulation and Strouhal number. Applying (3.5) to these low-Reynolds-number data yields a similar collapse as shown in figure 3(*c*), but with a mean value of about 35 instead of 58. The difference is attributed to the viscous nature of the low-Reynolds-number flow in which the boundary layer thickness is comparable to the peak-to-peak amplitude of the trailing edge. We anticipate that other factors will

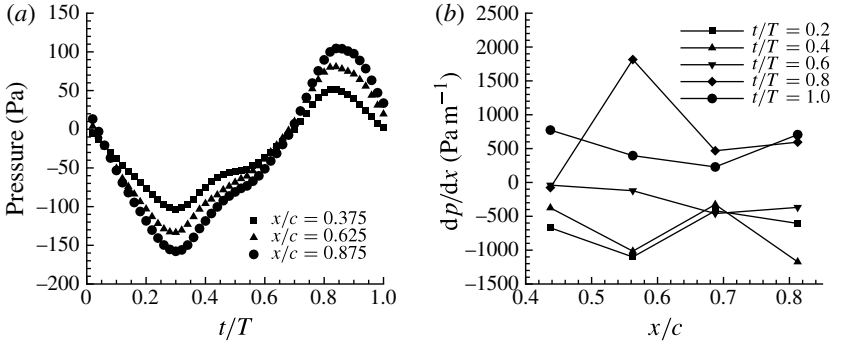

FIGURE 4. (*a*) Phase-averaged pressure variation over one cycle for $AR = 0.54$, $A/S = 0.31$ and $St = 0.27$ at varying chordwise measurement locations; (*b*) streamwise pressure gradient on the symmetry plane ($St = 0.27$).

change the value of the parameter, such as planform and cross-sectional shape, and the nature of the motion (e.g. pitch versus plunge).

The assumptions regarding pressure and pressure gradient on which (3.5) is based can be more rigorously assessed by considering the spatial and temporal variations in the surface pressure. Figure 4 shows the experimental data for case P1A2, where the measurements were acquired while the panel is advancing for $0 < t/T < 0.25$ and $0.75 < t/T < 1$. Figure 4(*a*) clearly shows that the amplitude of the pressure fluctuation increases toward the trailing edge of the panel for configuration P1A2 and so, locally, the assumed dependence of pressure on $(fA)^2$ is supported. However, whereas pressure was assumed to be driven by the transverse velocity, the pressure maxima occur at the extrema of the motion. This suggests that the pressure distribution is primarily an inertial response. According to ideal unsteady aerodynamic theory (Theodorsen 1935), forces governed by these inertial effects do not contribute to the bound circulation. Since flow separation causes significant deviation from the ideal flow assumptions on which the theory is based, it is difficult to separate non-circulatory forces, conceptually and quantitatively, from the circulatory forces. Nevertheless, the data suggest a strong inertial effect.

The pressure gradient $\mathrm{d}p/\mathrm{d}x$ was estimated at each time step using central differences at the mid-points between five pressure ports positioned on the panel symmetry line between $x/c = 0.375$ and 0.875 (see Green & Smits 2008 for details of the geometry and measurements). Surprisingly, at all three Strouhal numbers considered, the magnitude of the streamwise pressure gradient exhibits a consistent and significant variation, with chordwise position revealing maxima in $|\mathrm{d}p/\mathrm{d}x|$ at $x/c \approx 0.56$ for $t/T = 0.2, 0.4$ and 0.8 and minima at $x/c \approx 0.69$, as shown in figure 4(*b*). The pressure gradient distribution is reasonably robust as the panel advances, indicating that most of the spanwise vorticity is generated in a localized chordwise region. However, for $t/T = 0.6$ and 1.0, when the transverse velocity is large, the magnitude of $\mathrm{d}p/\mathrm{d}x$ is much smaller and deviates from the distributions seen more frequently near the extrema of the transverse displacement. There does not appear to be a direct relationship between instantaneous transverse velocity and vorticity flux, even though the kinematic scaling of (3.3) suggests a primary dependence on the panel transverse velocity. We will now show, however, that when we consider the vorticity flux due to pressure gradient integrated in space and time, we find the required support for the proposed scaling.

P1A2 (DPIV)		P1A2 (4.1)		P1A4 (4.1)	
St	Γ	St	Γ	St	Γ
0.18	0.0150	0.17	0.0163		
0.28	0.0156	0.27	0.0166	0.27	0.0365
0.47	0.0138	0.44	0.0171	0.44	0.0400
Mean	0.0148		0.0167		0.0383

TABLE 2. Comparison of wake circulation Γ ($m^2\ s^{-1}$) between measured values and values calculated according to (4.1) in one half-cycle. The flow cases are given in table 1. Note that there are slight differences in Strouhal number between the DPIV and pressure measurements.

4.2. *Pressure distribution and vorticity flux*

On the symmetry plane, (3.1) can be integrated over one half-cycle to predict the circulation shed in that stroke. Due to the symmetry of the motion, the integration may instead be evaluated on one side of the panel for the complete cycle,

$$\Gamma = -\frac{1}{\rho}\int_0^{T/2}\int_0^{C}\frac{\partial p}{\partial x}\,\mathrm{d}x\,\mathrm{d}t\bigg|_1 - \frac{1}{\rho}\int_0^{T/2}\int_0^{C}\frac{\partial p}{\partial x}\,\mathrm{d}x\,\mathrm{d}t\bigg|_2 \approx \frac{1}{\rho}\int_0^{T}\int_0^{C}\left|\frac{\partial p}{\partial x}\right|\,\mathrm{d}x\,\mathrm{d}t, \quad (4.1)$$

where we assume a pressure gradient of constant sign during a single stroke, and the subscripts 1 and 2 distinguish the sides of the panel. Since the panel is instrumented between $x/c = 0.375$ and 0.875, the integration is conducted only over this spatial extent.

Evaluating (4.1) discretely with $\Delta t/T = 0.02$ for case P1A2 yields the circulation values shown in the middle column of table 2 for one half-cycle. The pertinent beginning and end points of the half-cycle are defined by the change in sign of the vorticity shed into the wake. Since the time integration in (4.1) is conducted over a whole cycle, this distinction is not relevant for the pressure data. The mean circulation values computed by integration of the pressure gradients are within approximately 12 % of the DPIV measurements given in the first column. This is not necessarily expected since the computed circulations are based on measurements over only half of the panel chord. Figure 4(*b*), however, indicates that $|\mathrm{d}p/\mathrm{d}x|$ is generally decreasing at the most upstream measurement, so it is likely that it would be small further upstream where the displacements are small. It is also plausible that the pressure gradient upstream of this point is balanced by a pressure gradient of opposite sign near the trailing edge in order to relieve the pressure acting on the panel, as discussed in Green & Smits (2008). As to the dependence on Strouhal number, the DPIV data and the circulation values computed using pressure gradients are nearly invariant with Strouhal number: the maximum deviation from the mean is 2.4 and 6.8 % for the pressure- and DPIV-based measurements, respectively. Table 2 also lists circulation values computed from the pressure data for configuration P1A4, in which the frequency is the same as P1A2 and the amplitude is doubled so that the resulting circulation values would be expected to increase by a factor of approximately 2.37 according to (3.5). The ratio of circulation for P1A4 to P1A2 derived from pressure gradients using (4.1) is approximately 2.29, validating the scaling for values of A/S that are larger than previously considered.

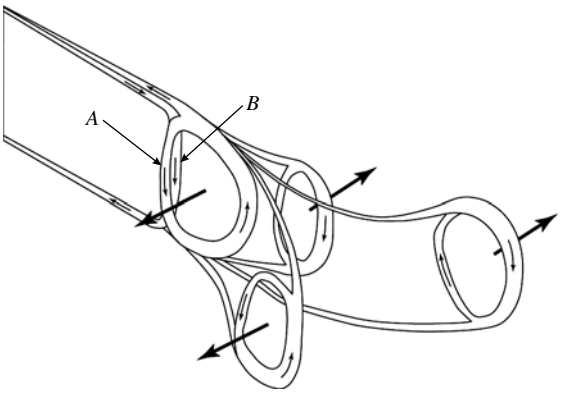

FIGURE 5. Vortex skeleton model proposed by Buchholz & Smits (2008), highlighting two adjacent, like-signed vortices shed from the trailing edge.

4.3. *Relation to vortex formation number and vortex topology*

The formation number n of a piston-formed vortex ring is defined by $n = Ut/D$, where U is the piston velocity, t is dimensional time, and D is piston diameter (Gharib, Rambod & Shariff 1998). It is a dimensionless parameter governing pinch off of the vortex ring such that beyond $n \approx 4$ no additional vorticity is entrained. Dabiri (2009) proposed that the formation number of a vortex ring can be expressed by a non-dimensional circulation $\hat{T} \propto \Gamma/(D\Delta U)$, where the length and velocity scales D and ΔU are determined from the kinematics and geometry of the problem. The role of formation number in the flow dynamics and performance of wings and fins has been demonstrated by Milano & Gharib (2005), Ringuette, Milano & Gharib (2007), Rival, Prangemeier & Tropea (2009), Taira & Colonius (2009) and Chen, Colonius & Taira (2010), and Dabiri (2009) postulated that formation number may govern forward locomotion by periodically oscillating wings or fins. There is limited evidence for this claim, although Rival *et al.* (2009) showed that application of Dabiri's formulation yields a useful scaling for the maximum circulation of the leading-edge vortex produced by an aerofoil plunging with uniform amplitude and reduced frequency.

For the wakes investigated here, formation number must be interpreted in the appropriate context. While the transition from a von Kármán-like wake as in figure 2(*c*) to a bifurcating wake, such as those shown in figure 2(*a,b*), seems a plausible manifestation of the pinch-off process in a two-dimensional sense, one must take into account the history of vortex shedding and the constraints imposed by the solenoidal condition on the vorticity field. For example, the wake model presented by Buchholz & Smits (2008) asserts that the two adjacent like-signed vortices shed in one stroke are components of distinct vortex ring structures, as shown in figure 5. According to this model, the first spanwise vortex to be shed in the stroke, labelled A, is connected to a vortex ring that was initiated in the previous stroke, and is therefore part of a pre-existing downstream structure. In contrast, vortex B is connected to a new upstream structure still in the process of being shed by the panel. While viscous effects may allow diffusion and reconnection of structures, their origins make them fundamentally distinct. Therefore the strength of vortex A is pre-defined and the division between A and B is not directly related to a formation-number-governed pinch-off phenomenon.

Since (3.5) relates the total circulation shed in one half-cycle to the kinematic and geometric variables governing the creation of that circulation, and the shed circulation consists of more than one vortex structure, (3.5) does not perform the role of a formation number in the present context. Rather, it is a complementary parameter in the general case where both parameters may be relevant. For example, formation number may govern the strength of a single vortex ring structure whereas the proposed parameter would govern the total shed circulation. Whether or not vortex pinch-off occurs, (3.5) provides a useful scaling of the total vorticity shed in a stroke. It provides an important bound that can be used to help quantify existing wake structure models and inform low-order unsteady aerodynamic models.

Nevertheless, for an appropriate circulation measurement, interpreting (3.5) as a formation number seems plausible. For example, Rival *et al.* (2009) showed that $\hat{T}$ applied to the leading-edge vortex of their plunging aerofoil exhibits considerably reduced scatter when computed using $D = 2c = 4h_0$ and $\Delta U = 2\pi f h_0$, compared to the dimensional circulation. Their expression for formation number, $\hat{T} = \Gamma/(8\pi f h_0^2)$, is completely analogous to (3.3). Thus, it is possible that (3.5) may be applied to individual vortex structures, and perform the role of a three-dimensional formation number for periodic flows. It is also noteworthy that, if the formation number formulation of Dabiri (2009) ($\hat{T}$) is implemented in the present work with $D = 4AS/(2A + 2S)$ (the hydraulic diameter of the peak-to-peak projection of the panel in the streamwise direction) and $\Delta U = fA$, we arrive at (3.5) with $\beta = 1$. The resulting variability in $\hat{T}$ is $\sigma_{\overline{\Gamma}} = 0.082$, which is approximately 17 % larger than for (3.5) with $\beta = 7$.

5. Conclusions

A new scaling parameter is proposed for the circulation shed by finite-aspect-ratio, rigid, rectangular panels pitching about their leading edges. The parameter is the product of a kinematic scaling, and a geometric scaling based on the work of Green & Smits (2008). The underlying tenet guiding the development of the parameter is that in periodic, symmetric motion, the circulation shed by the panel in a stroke or half-cycle must be equal to the circulation generated during that interval by pressure gradients acting on the surface. The parameter yields an approximately constant value with variations in panel aspect ratio, pitching amplitude, and Strouhal number for low-aspect-ratio panels at $Re_C = O(10^4)$, and thereby provides a useful bound for quantitative prediction of wake properties. It is postulated here that the proposed parameter may either complement or replace formation number in the quantitative description of unsteady wakes. It was also suggested that in some applications, this parameter may be equivalent to a three-dimensional formation number for periodic flows.

Acknowledgements

A.J.S. acknowledges the support of the Office of Naval Research under MURI grant number N00014-08-1-0642. J.H.J.B. acknowledges the support of the Air Force Office of Scientific Research under grant number FA9550-11-1-0019.

REFERENCES

ANDERSON, J. M., STREITLIEN, K., BARRETT, D. S. & TRIANTAFYLLOU, M. S. 1998 Oscillating foils of high propulsive efficiency. *J. Fluid Mech.* **360**, 41–72.

BORAZJANI, I. & SOTIROPOULOS, F. 2010 On the role of form and kinematics on the hydrodynamics of self-propelled body/caudal fin swimming. *J. Expl Biol.* **213**, 89–107.

BUCHHOLZ, J. H. J. & SMITS, A. J. 2006 On the evolution of the wake structure produced by a low-aspect-ratio pitching panel. *J. Fluid Mech.* **546**, 433–443.

BUCHHOLZ, J. H. J. & SMITS, A. J. 2008 The wake structure and thrust performance of a rigid low-aspect-ratio pitching panel. *J. Fluid Mech.* **603**, 331–365.

CHEN, K. K., COLONIUS, T. & TAIRA, K. 2010 The leading-edge vortex and quasisteady vortex shedding on an accelerating plate. *Phys. Fluids* **22**, 033601.

DABIRI, J. O. 2009 Optimal vortex formation as a unifying principle in biological propulsion. *Annu. Rev. Fluid Mech.* **41**, 17–33.

DONG, H., MITTAL, R. & NAJJAR, F. M. 2006 Wake topology and hydrodynamic performance of low-aspect-ratio flapping foils. *J. Fluid Mech.* **566**, 309–343.

GHARIB, M., RAMBOD, E. & SHARIFF, K 1998 A universal time scale for vortex ring formation. *J. Fluid Mech.* **360**, 121–140.

GREEN, M. A. & SMITS, A. J. 2008 Effects of three-dimensionality on thrust production by a pitching panel. *J. Fluid Mech.* **531**, 211–220.

KOOCHESFAHANI, M. M. 1989 Vortical patterns in the wake of an oscillating aerofoil. *AIAA J.* **27** (9), 1200–1205.

LIGHTHILL, M. J. 1963 Introduction boundary layer theory. In *Laminar Boundary Layers* (ed. L. Rosenhead), pp. 46–113. Oxford University Press.

MILANO, M. & GHARIB, M. 2005 Uncovering the physics of flapping flat plates with artificial evolution. *J. Fluid Mech.* **534**, 403–409.

RINGUETTE, M. J., MILANO, M. & GHARIB, M. 2007 Role of the tip vortex in the force generation of low-aspect-ratio normal flat plates. *J. Fluid Mech.* **581**, 453–468.

RIVAL, D., PRANGEMEIER, T. & TROPEA, C. 2009 The influence of aerofoil kinematics on the formation of leading-edge vortices in bio-inspired flight. *Exp. Fluids* **46**, 823–833.

TAIRA, K. & COLONIUS, T. 2009 Three-dimensional flows around low-aspect-ratio flat-plate wings at low Reynolds numbers. *J. Fluid Mech.* **623**, 187–207.

THEODORSEN, T. 1935 General theory of aerodynamic instability and the mechanism of flutter. NACA. *Report* 496.

TRIANTAFYLLOU, M. S., TRIANTAFYLLOU, G. S. & YUE, D. K. P. 2000 Hydrodynamics of fishlike swimming. *Annu. Rev. Fluid Mech.* **32**, 33–53.

WU, J. Z. & WU, J. M. 1993 Interactions between a solid surface and a viscous compressible flow field. *J. Fluid Mech.* **254**, 183–211.

WU, J. Z. & WU, J. M. 1996 Vorticity dynamics on boundaries. In *Advances in Applied Mechanics* (ed. J. W. Hutchison & T. Y. Wu), vol. 32. pp. 119–275. Academic.

YOUNG, J. & LAI, J. C. S. 2007 Vortex lock-in phenomenon in the wake of a plunging aerofoil. *AIAA J.* **45** (2), 485–490.